Modeling the Design of Plasmonic Biosensor Device by using Abstract Finite State Machine Model and FDTD Based MEEP Tool

Divya Sharma, R.P.Dwivedi

Abstract: *This paper describes and highlights the usage of Finite State Machine (FSM) M' model using the Finite Automata sub-systems (M'$_1$, M'$_2$, M'$_3$, ...,M'$_n$) for a nanoscale biosensor sub-block system design which accepts the languages L'$_1$ to L'$_n$ individually or a common language L'. The biosensor sub-block design and development is a challenging task, as it involves solving complex sub-blocks operations and the Finite Automata design tools provide the different approaches to address the same. Here each sub-system of the biosensor system is individually modeled using Finite Automata and they are simulated by using Massachusetts Institute of Technology Electromagnetic Equation Propagation (MEEP) tool, to model the structure and Plasmonic behavior of the device. The individual sub-system can be mathematically modeled using the MATLAB Simulink as FSM and finally combined to form a target complex biosensor device as well as complete biosensor system. The objective of this paper is to showcase the usage of FSM simulation in the development of biosensor devices as a part of Plasmonic biosensor device design process.*

Index Terms: *Biosensors, Finite State Machine, Massachusetts Institute of Technology Electromagnetic Equation Propagation tool (MEEP), Nanotechnology, Plasmonics.*

I. INTRODUCTION

The nanotechnology finds its application in many key areas like in the design and development of biosensor devices for medical diagnostics [1], [2], fabrication of microprocessor in computing industry, solar panel optimization in renewable energy sector, communication devices [3] etc. It is one of the most expensive area of research under which the cost of translating the design and fabrication from initial requirements to the final end product is very high and time consuming [4], [5]. This high cost can limit the development of new nanotechnology based Plasmonic biosensors devices [6]–[9]. Here the main challenge is to mitigate the complexity of design and development of a biosensor device [10]–[12]. The simplification in the design and development process would significantly help the researchers to accelerate and perform iterative experimental research to re-validate the claims, findings and the research outcomes by using various simulation tools. In this paper,

the Finite Automata design tools are used in the design and modeling of a nanoscale biosensor device before the actual fabrication takes place. This design approach is significantly different from the existing design process like MEEP [13], [14] or Discrete Dipole Scattering (DDSCAT) simulation tools. Here Finite Automata design tools provide different levels of abstraction and other unique approaches, which would help in modelling of the biosensor device easily.
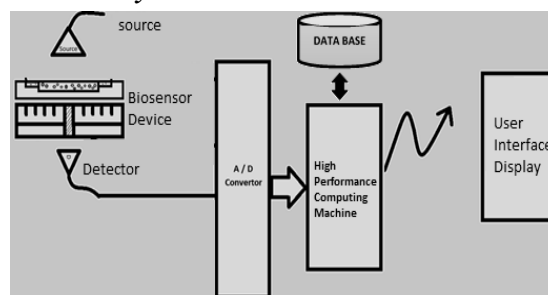
A. Biosensor System

Fig. 1 Biosensor system block diagram.

A biosensor is a device with associated support system which can be used to sense and quantify biological components for example glucometer is used to measure the glucose level [15]. The biosensor device can be designed and developed based on optical, physicochemical, electrochemical and piezoelectric principles. The biosensor device is generally coupled with the complex allied electronic sub-system as shown in the Fig. 1 to enhance, measure and provide the results in user-friendly format. These electronics sub-system includes the light source as the input unit and the detector unit for capturing the changes in the physical parameters of light that attributes to the biosensor device with target specimen. These captured signals are digitized using high precision and high-speed Analog to Digital (A/D) convertor and fed into artificial intelligence based high performance computing machine, which is backed up by the training of database to compute and provide the necessary results. These state-of-art biosensor machines can be easily designed and modelled using Finite State Machine model as a whole unit shown in Fig. 1 or only as the electronics sub-system and the nanoscale biosensor sensor device [16], [17]. Here, the focus is on the nanoscale biosensor's design and modeling.

B. Finite State Automata System
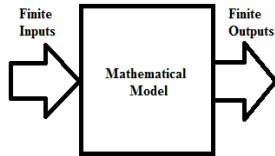
Fig. 2 Finite state automata with finite inputs and finite outputs.

The Finite State Automata (FSA) Fig. 2 is a Finite State Machine (FSM) which models the computation mathematically. The FSA is an abstract machine which accepts finite set of inputs and provides finite set of outputs with finite set of states. The transition function 'δ' is used to make the transition of FSM from one state to another based on the inputs. The Fig. 2 is a mathematical model of any system with finite inputs and finite outputs. The set $\{ I_1, I_2, …. I_q \}$ marks as the finite set of inputs with fixed values and the set $\{ O_1, O_2, …. O_q \}$ as the finite set of outputs with fixed values. This mathematical model can be used to model any kind of system and sub-systems. The finite state machine with output model is formally defined as six tuples machine,

$$M = \{\textstyle\sum, O, Q, \delta, X, q_o\}$$

(1)

Where,

- $\sum$ – Input Alphabet
- O – Output Alphabet
- Q – Finite set of states
- qo– Initial state
- δ – Transition Function: Q X $\sum$ → , the state q from a finite state set Q upon an input symbol from the input alphabet $\sum$, makes a transition into state which is again from the same set Q.
- X – Transition Function: Q X $\sum$ → , the state q from a finite state set Q upon an input symbol from the input alphabet $\sum$, ejects an output symbol from output alphabet O.

Here the key aspect is that the input and outputs of the FSM can be easily used to map the biosensor's device input and output as languages. These unique approach opens up to model any kind of system and sub-systems of biosensor devices as described in the Sec. II as Finite State Machines.

II. GENERIC BIOSENSOR MACHINE OR SYSTEM OR DEVICE BLOCK DESIGN APPROACH
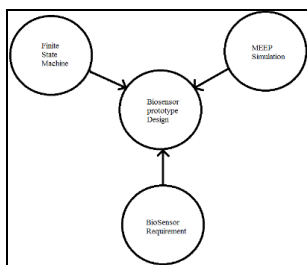
Fig. 3 Biosensor prototype design approach using FSM and MEEP simulation model.

The approach of design and developing generic biosensor

device prototype is shown in the Fig. 3. The MEEP is an open-source command line script programming language based on the FDTD method for simulation of electromagnetic equation propagation [18]. This tool with the aid of allied tools like h5tools, mayavi2 [19] can be used to simulate the structural and behavioral functions of nanoscale biosensor devices. Here the FSM design tools and the MEEP simulation tools are used to translate the biosensor requirements into virtual biosensor device design as described in the Sec 2.1 design process flow.

A. Algorithm: Design Process Flow

Step 1: Start

Step 2: User specified target biosensor device or system requirement.

Step 3: Simulation of the biosensor device using MEEP tool.

Step 4: Simulation of the biosensor device using FSM design tool.

Step 5: Comprehend the biosensor device behavior using MEEP and FSM simulation model.

Step 6: If design refining is required: go to step 2 else go to step 7.

Step 7: Initiate the physical biosensor device fabrication in fab labs.

Step 8: Stop.

The paper focuses and emphasis on the steps 3, 4 and 5 which forms a crucial stage for the design of biosensor device. A case study of biosensor device block with circular channel waveguide design has been investigated using MEEP and FSM simulations.

III. EXPERIMENTAL SETUP FOR BIOSENSOR DEVICE WITH CIRCULAR WAVEGUIDE SIMULATION USING MEEP AND FSM

The MEEP simulation hardware setup includes the machine details: AMD A10-7850K APU processor with 4 CPU cores and 8 GPU cores operating at frequency 4.1GHz, RAM configuration details: 16 Giga bytes with speed 1600MHz. The secondary storage hard disk drives: 500 Gigabytes and one Terabytes and finally the BIOS Settings: Version-A88X-BIOS (2502). Software Setup includes: Ubuntu 14.04.4 LTS AMD64 Operating System with the Linux kernel (3.19.0-49-generic x86_64). The MEEP simulation tool and allied visualization tools include, MEEP 1.1.1, libctl 3.1, Guile 1.8.8, MPI version 2.1.1, mpirun (Open MPI) 1.6.5, HDF5 utils, h4fromh5, h5fromh4, h5fromtxt, h5math, h5topng, h5totxt, h5tovtk and MayaVi 4.1.0. General system configuration requires system stack size marked as unlimited and swap size ~701 Giga Bytes.For the FSM simulation, the hardware setup is same as MEEP simulation hardware configuration but software setup includes the following details: Windows 10 (64 bit) operating system. The development and simulation tools: Visual studio 2015, MATLAB 9.2 (R2017a) and Simulink.

A. Biosensor Device Model Specification Details

The sample sensor example with two material types are silver as metal (M) layer and air as insulator (I) layer for the simulation of Metal-Insulator-Metal (MIM) structure. The insulator layer is sandwiched between the metal layers and a central hole runs through all the layers. The two concentric waveguides patterned are formed on the top of silver layer block as shown in Fig. 6.1.The following are the biosensor specification in three-dimension quadrant (x, y, and z) with a central groove,

- Lattice size (x, y, z) = (10,10,10)
- block size (x, y, z) = (5, 0.25, 5)
- MIM structure = Silver – Air – Sliver
- Central hole : Radius = 0.15, Height = infinity
- Concentric waveguide pattern:
  - Waveguide 1: Radius = 1.65, Height = 0.25
  - Waveguide 2: Radius = 1.15, Height = 0.25
  - Waveguide 3: Radius = 0.85, Height = 0.25
- Perfectly matched layer = 1.0
- Number of frequencies at which to compute flux : 100
- The following are the run source specification,
  - Source = gaussian-source
  - Pulse center frequency = 0.15
  - Pulse width = 0.1

B. Circular Waveguide-Based Biosensor Sub-System Machine with and Without Central Grooves
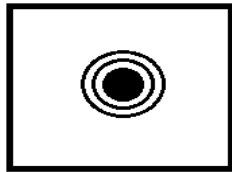

Fig. 4.1 Biosensor block with the central groove and concentric waveguide
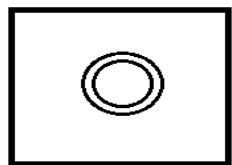

Fig. 4.2 Biosensor block without the central groove and with concentric waveguide

The biosensor device or machine M' is proposed with the central cylinder and two concentric waveguides Fig. 4.1 and structured with layer of Metal-Insulator-Metal (MIM) heterogenous structure. The second biosensor device or machine M'' Fig. 4.2 is proposed without the central cylinder but with the same dimensions of two concentric waveguides as in Fig. 4.1 and structured with layer of the Metal-Insulator-Metal (MIM) heterogenous structure to be simulated using FSM model.

C. Mathematical Model of FDTD Method

In FDTD method, the transmitted power through custom structure design for the given frequency ω, is the integral of the Poynting vector (in the normal n^n^ direction) over a plane is given by the equation:

$$P(w) = R_e \hat{n} \int E_w(x)^* H_w(x) d^2 x$$

(2)

Similarly, for the reflected power through custom structure design for the given frequency, the reflected power is obtained by subtracting the Fourier-transformed incident fields E(0)ω(x) and H(0)ω(x) in the below equation:

$$P_r(w) = R_e \hat{n} \int [E_w(x) - E_w^{(0)}(x)][H_w(x) - H_w^{(0)}(x)] d^2 x$$

(3)

IV. DETAILED MEEP SIMULATIONS OF BIOSENSOR SYSTEMS MACHINE WITH CIRCULAR WAVEGUIDE WITH AND WITHOUT CENTRAL GROOVE

The MEEP provides a set of geometric-object constructs that can be used for building the sensor block structure. The basic geometric structure includes cylinder, block, sphere, cone, ellipsoid, etc. It provides basic constructs to specify the type of material like gold, silver, etc. and finally it also supports various types of source settings to simulate the electromagnetic wave propagation. Here the devices Fig 4.1 and Fig 4.2 are the simulations using MEEP.

A. Simulation Results for The Circular Waveguide Biosensor with and Without Central Grooves

The MEEP provides the simulation output in the form of Hierarchical Data Format 5 (HDF5) [19] files which can be used by the visualization tools like h5utils to extract data and visualize the structures. Here the h5topng and h5tovtk sub tools of h5utils are used to extract and store the information in the form of 'png' image and 3D 'vtk' file format respectively. The 3D visualizing tool MayaVi2 can be used to visualize the sensor block structure in 3D. The sample example of output of MayaVi2 is as shown Fig. 5 and Fig. 6.

B. Simulation Results for the Circular Waveguide Biosensor with and without Central Groove

The structural simulation of the circular wave guide biosensor device with circular central groove using MEEP is shown in the Fig. 5 (a) (b) (c) and (d). Similarly, the Fig. 6 (a) (b) (c) and (d) shows the structural simulation of the circular wave guide biosensor device without circular central groove.
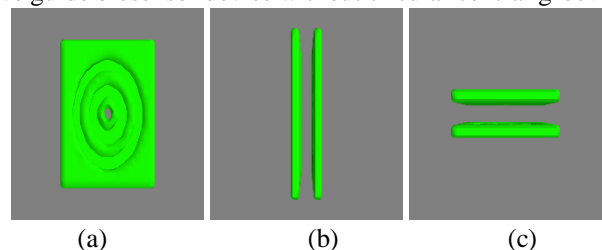

(a)   (b)   (c)
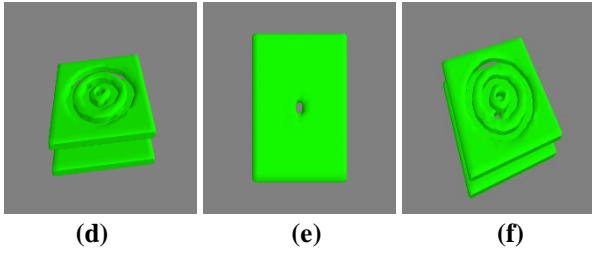
Fig. 5 Circular waveguide biosensor with central grooves: (a) top view (b) vertical side view (c) horizontal side view (d) angled view1 (e) bottom view and (f) angled view2
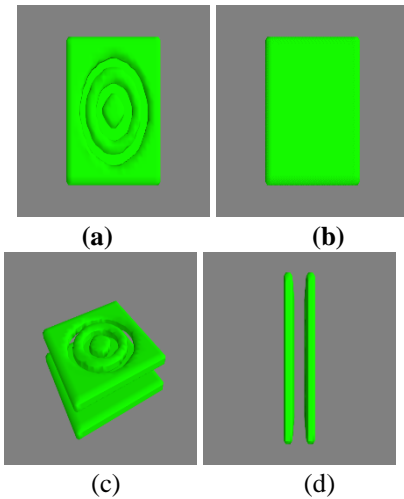
Fig. 6 Circular waveguide biosensor without central grooves: (a) top view (b) bottom view (c) angled view and (d) vertical side view

C. Simulation Graphs Results for the Circular Waveguide Biosensor with and without Central Groove

The behavior simulation is performed twice, once with the central groove and the other is without the central groove, the flux spectra is computed by using the runtime specification with source as gaussian-source, Pulse center frequency at 0.15 and Pulse width set to 0.1 as input for transmission, reflection flux and the loss output data points. The output data points are marked in the Appendix I and II with the associated chart plots are marked as in the Fig. 7, Fig. 8, Fig. 9, Fig. 10 and Fig. 11. The Fig.7 shows the circular waveguide frequency Vs loss, the device shows the damping of loss as the frequency increases.
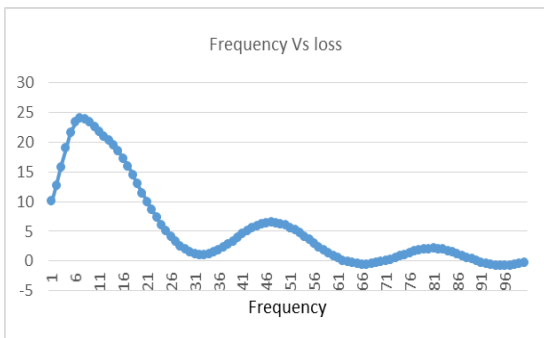
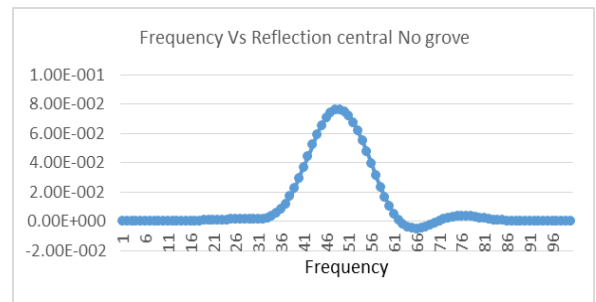**Fig. 7 MEEP results - Circular waveguide-Frequency Vs Loss**

The Fig.8 shows the circular waveguide with cylinder with frequency Vs reflection, the device shows the Gaussian behavior.
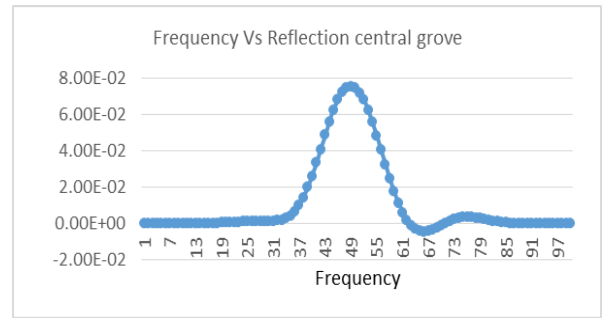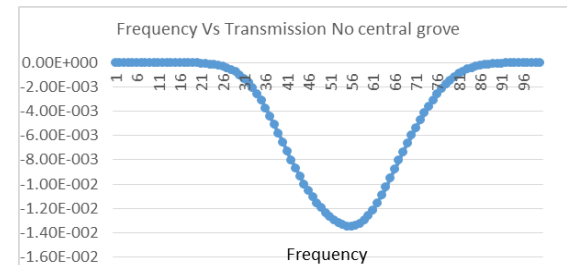

Fig. 8 MEEP results - Circular waveguide frequency Vs Reflection with Cylinder

The Fig.9 shows the circular waveguide without central grove cylinder with frequency Vs reflection, the device shows the Gaussian behavior.
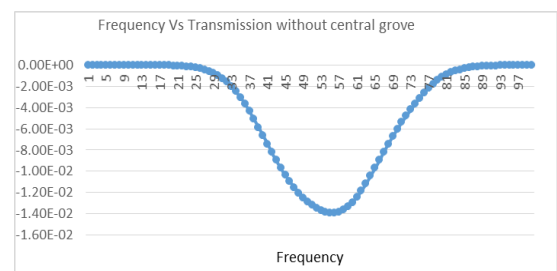

Fig. 9 MEEP results - Circular waveguide Frequency Vs Reflection without Cylinder

The Fig.10 shows the circular waveguide with central grove cylinder with frequency Vs transmission, the device shows the negative Gaussian behavior.

Fig. 10 MEEP results - Circular waveguide Frequency Vs Transmission with Cylinder

The Fig.11 shows the circular waveguide without cylinder with frequency Vs transmission, the device shows the inverse Gaussian behavior.

Fig. 11 MEEP results - Circular Waveguide - Frequency Vs Transmission without Cylinder

V. FINITE STATE MACHINE MODEL OF BIOSENSOR DEVICE M'

The generic biosensor system and sub-systems can be modelled as FSA machine M'. The biosensor system as a finite state machine M' would accept the input formal language L_i' and produce the output language Lo' respectively. The input language L_i' is generally defined based on the quantities in Eq. 2 and the output language L_o' is generally defined based on the quantities in Eq. 3,

Input Language L_i' = { frequency$_i$, wavelength$_i$, intensity$_i$, phase$_i$, angle$_i$, SourceType }

(2)

Where,

- Frequency$_i$: It is the operating input frequency range.
- Amplitude$_i$: It is the operating input amplitude range.
- Wavelength$_i$: It is the operating input wavelength range.
- Phase$_i$: It is the input phase value.
- Angle$_i$: It is the input angle value.
- SourceType : It is the input continuous or Gaussian source type.

Output Language L_o' = { frequency$_o$, wavelength$_o$, intensity$_o$, phase$_o$, angle$_o$, SourceType }

(3)

Where,

- Frequency$_o$:It is the operating output frequency range.
- Amplitude$_o$:It is the operating output amplitude range.
- Wavelength$_o$:It is the operating output wavelength range.
- Phase$_o$: It is the output phase value.
- Angle$_o$: It is the output angle value.

The biosensor sub-systems are modelled as an individual Finite State Machine M_1', M_2', M_3', M_4', M_5',....M_n' which accepts the input language L_{i1}', L_{i2}', Li3', Li4', Li5',…. Lin' and releases the output languages as Lo1', Lo2', Lo3', Lo4', Lo5',…Lon' respectively. This biosensor machine sub-system blocks would also require an interfacing sub-block if there are two or more sub-blocks, which has a disjoint language Lix' acceptance. These languages would be treated as the interfacing languages or mapper languages which are accepted by the interfacing sub-blocks.
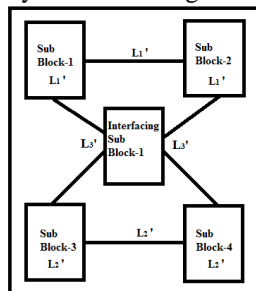

Fig. 12 Generic model M of Biosensor with M_1', M_2', M_3', and M_4' sub-blocks with the M_5' interfacing sub-block

The Fig. 12 machine M has the sub-blocks 1, 2, 3, 4 and an interfacing sub-block 1. The sub-blocks 1 and 2 accepts the input language L_1' Eq. 4, the interfacing block accept L3' Eq. 5, and the sub-blocks 3 and 4 accepts the input language L_2' Eq. 4. The interfacing sub-block accepts the interfacing language L_3' Eq. 5, which acts as the interfacing or mapping language between sub-blocks 1, 2 and 3, 4.

Input/output Language $L_1'$and L_2' = {frequency$_{io}$, wavelength$_{io}$, intensity$_{io}$, phase$_{io}$, angle$_{io}$, Gaussian mode$_i$ or continuous model$_i$}

(4)

Interfacing Language L_3' = {frequency$_{interface}$, wavelength$_{interface}$, intensity$_{interface}$, phase$_{interface}$, angle$_{interface}$, Gaussian model$_{interface}$ or continuous model$_{interface}$}

(5)

A. Biosensor Device M' Design using Finite State Machine

Fig. 13 Generic Plasmonic Biosensor using Finite State Machine M' by Integrating C-Code in State flow using Simulink

The Fig. 13 describes the generic biosensor block and sub-blocks which models the mathematical transformation equations accepting or rejecting the formal language L'. The Fig.13 describes the following details of sub-blocks of the Finite State System.

- Input: Gaussian source.
- 5 Sub-blocks of FSM
  - Transmission sub-blocks FSM
  - Reflection sub-block FSM
  - Loss sub-block FSM
- Input and Output scopes to monitor the behavior (scope$_1$, scope$_2$, scope$_4$ and scope$_6$).

B. Biosensor Sub-systems Machine with Central Groove FSM based Model M'

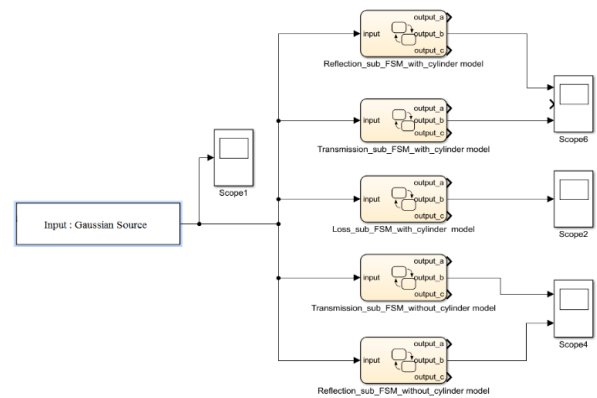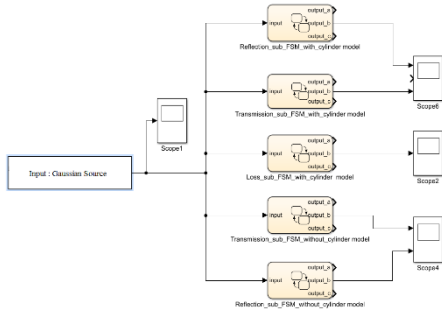**Fig. 14 Circular waveguide Plasmonic Biosensor with and without central cylinder using Finite State Machine by Integrating C-Code in State flow using Simulink**

The Fig. 14 describes the generic biosensor block and sub-blocks which models the mathematical transformation equations accepting or rejecting the formal language L'. It is modelled for both the with and without central groove,

- Input: Gaussian source.
- Sub-blocks of FSM
- Here transmission sub-block FSM, the transmission Vs input frequency is modelled.
- Here the reflection sub-block FSM, the transmission Vs input frequency is modelled.

The loss is modelled based on with and without central groove Loss sub-block FSM. The input and output scopes monitor the behavior.

C. Mathematical Model and the Chart Plot of the FSM based Biosensor Device Behavior

The sub-section D to sub-section H describes the circular waveguide with and without central groove for biosensor sub-system's mathematical model equations. These equations are extracted using the curve fitting of the chart plots Fig. 7, Fig. 8, Fig. 9, Fig. 10, Fig. 11 and these equations are then injected into the FSM by integrating C-code into state flow machine, using Simulink for both circular waveguide with and without central cylinder groove for Plasmonic biosensor device behaviour. The significance of these equations is that they fundamentally model the same biosensor device's reflection, transmission and loss properties which can be easily integrated into FSM computing model as part of the design process of the biosensor device. The simulation results of the circular waveguide-based biosensor sub-system's FSM model. The measured fluxes for transmission, reflection fluxes and the losses with the Gaussian source as the input are shown in the chart plot Fig. 15, Fig. 16, Fig. 17, Fig. 18 and Fig. 19.

D. Circular Waveguide: Frequency Vs Loss Equation

The polynomial Eq. 6 is obtained by the curve fitting in MATLAB using the data points of frequency Vs Loss chart plot. It shows the damping behavior as the frequency increases.
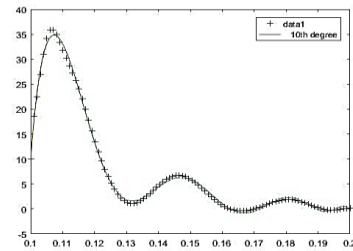
$$y = P_1(x^{10}) + P_2(x^9) + P_3(x^8) + P_4(x^7) + P_5(x^6) + P_6(x^5) + P_7(x^4) + P_8(x^3) + P_9(x^2) + P_{10}(x) + P_{11}$$

(6)

Where,

- Coefficients: $P_1 = -3.5698e+15$, $P_2 = 5.2519e+15$, $P_3 = -3.451 + 2e+15$, $P_4 -= 1.334e+15$,

$P_5 = -3.3586e+14$, $P_6 = 5.7565e+13$,
$P_7 = -6.8034e+12$, $P_8 = 5.4768e+11$,
$P_9 = -2.8753e+10$, $P_{10} = 8.8948e+08$,
$P_{11} = -1.2321e+07$

- Norm of residuals = 4.9934

Fig. 15 Circular waveguide-Frequency Vs Loss

E. Circular Waveguide with Cylinder: Frequency Vs Reflection Equation

The polynomial Eq. 7 is obtained by the curve fitting in MATLAB using the data points of frequency Vs reflection chart plot of circular waveguide with central cylinder. It shows the positive Gaussian behavior.

$$y = P_1(x^{10}) + P_2(x^9) + P_3(x^8) + P_4(x^7) + P_5(x^6) + P_6(x^5) + P_7(x^4) + P_8(x^3) + P_9(x^2) + P_{10}(x) + P_{11}$$

(7)

Where,

- Coefficients: $P_1 = -4.9434e+13$, $P_2 = 7.3703e+13$,
  $P_3 = -4.9111e+13$, $P_4 = 1.9257e+13$,
  $P_5 = -4.9202e+12$, $P_6 = 8.5584e+11$,
  $P_7 = -1.0264e+11$, $P_8 = 8.3788e+09$,
  $P_9 = -4.4563e+08$, $P_{10} = 1.3943e+07$,
  $P_{11} = -1.9491e+05$
- Norm of residuals = 0.057416

Fig. 16 Circular waveguide Frequency Vs Reflection with cylinder
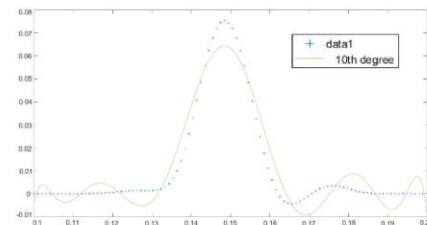
F. Circular Waveguide with Cylinder: Frequency Vs Reflection Equation

The polynomial Eq. 8 is obtained by the curve fitting in MATLAB using the data points of frequency Vs Reflection chart plot of circular waveguide without central cylinder. It shows the positive Gaussian behavior.

$$y = P_1(x^{10}) + P_2(x^9) + P_3(x^8) + P_4(x^7) + P_5(x^6) + P_6(x^5) + P_7(x^4) + P_8(x^3) + P_9(x^2) + P_{10}(x) + P_{11}$$

(8)

Where,
- Coefficients: P_1 = -4.9297e+13, P_2 = 7.3406e+13, P_3 = -4.8849e+13, P_4 = 1.9128e+13, P5 = -4.8804e+12, P_6 = 8.4771e+11, P_7 = -1.0151e+11, P_8 = 8.2743e+09, P_9 = -4.3939e+08, P_{10} = 1.3726e+07, P_{11} = -1.9157e+05
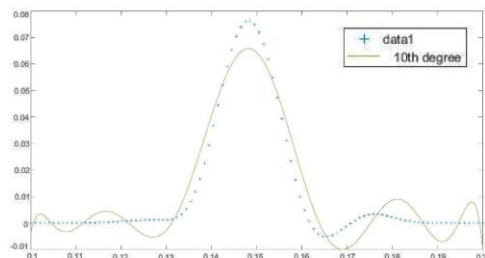- Norm of residuals = 0.057459

Fig. 17 Circular Waveguide - Frequency Vs Reflection without Cylinder

G. Circular Waveguide with Cylinder: Frequency Vs Transmission Equation

The polynomial Eq. 9 is obtained by the curve fitting in MATLAB using the data points of frequency Vs transmission chart plot of circular waveguide with central cylinder. It shows the negative Gaussian behavior.

$$y = P_1(x^{10}) + P_2(x^9) + P_3(x^8) + P_4(x^7) + P_5(x^6) + P_6(x^5) + P_7(x^4) + P_8(x^3) + P_9(x^2) + P_{10}(x) + P_{11}$$

(9)

Where,
- Coefficients: P_1= 1.1265e+12, P_2=-1.7304e+12, P_3=1.1862e+12, P_4=-4.7771e+11, P_5=1.2515e+11, P_6=2.2284e+10, P_7 = 2.7307e+09, P_8=-2.274e+08, P_9= 1.2316e+07, P_{10} = -3.9174e+05, P_{11} = 5558.3
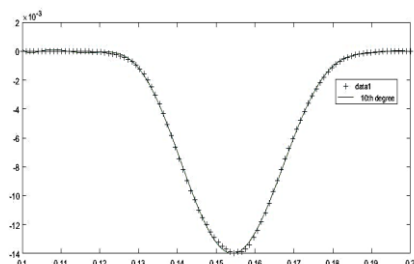- Norm of residuals = 0.0009477

Fig. 18 Circular Waveguide - Frequency Vs Transmission with Cylinder

H. Circular Waveguide without Cylinder: Frequency Vs Transmission Equation

The polynomial Eq. 10 is obtained by the curve fitting in MATLAB using the data points of frequency Vs transmission chart plot of circular waveguide without central cylinder. It shows the positive Gaussian behavior.

$$y = P_1(x^{10}) + P_2(x^9) + P_3(x^8) + P_4(x^7) + P_5(x^6) + P_6(x^5) + P_7(x^4) + P_8(x^3) + P_9(x^2) + P_{10}(x) + P_{11}$$

(10)

Where,
- Coefficients: P1 = 8.5306e+11, P2 = -1.3169e+12, P3 = 9.0668e+11, P4 = -3.6657e+11, P5 = 9.6358e+10, P6 = -1.7205e+10, P7 = 2.1133e+09, P8 = -1.7631e+08, P9 = 9.5624e+06, P10 = -3.0448e+05, P11 = 4323
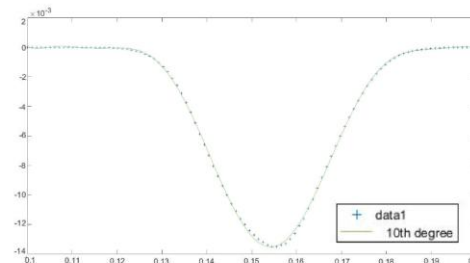- Norm of residuals = 0.00097021

Fig. 19 Circular Waveguide - Frequency Vs Transmission without Cylinder

VI. MEASUREMENT INFERENCE: FSM Vs MEEP MODELS SIMULATION

This paper develops the simulation model of biosensor using the two different approaches, one using the FSM and the another using MEEP based on FDTD model, for the transmission, reflection and the losses over the circular waveguide with or without the central cylinder groove. The two models using two different approaches for solving the design of the biosensor shows the similar pattern chart plots for both FSM and MEEP models. The circular waveguide's frequency Vs transmission with and without cylinder chart plot shows negative Gaussian. The circular waveguide's frequency Vs reflection with and without cylinder chart plot shows positive Gaussian. The model chart plot of circular waveguide losses follows the damping property. The importance of both the simulation models is that both can be used as a tool to understand the important parameters of transmission, reflection and loss for the given biosensor device. The measured results show similar behavior using both the MEEP and FSM simulation model, hence it can be seen that the FSM model can also be used as a simulation approach to design the biosensor device on the same lines of MEEP simulation model.

VII. CONCLUSION

The biosensor device and complete system design and development is very complex approach and exploring the legacy of powerful FSM as the abstract machine model, would help in reducing the complexity, simulation and design steps there by accelerating the different types of biosensor device development. The FSM design model applied to the biosensor device design and development process would help in the quick verification of the target biosensor device specification and its behaviour related to transmission, reflection and losses. Since it follows the machine abstraction, this approach can be applied to model other biosensor devices based on electrochemical, MEMS, piezoelectric principles to quantify other physical properties also. The FSM simulation model can be further expanded and explored to any of the biosensor device with different nanoscale patterns like Nano wells, Nano pyramids and others. Furthermore, future work exploration can be done on the FSM simulation of biosensor device which can also be integrated with the entire FSM of Artificial Intelligence based biosensor system model prototype.

APPENDIX

APPENDIX -I			
MEEP simulation: circular waveguide without central groove or cylinder flux as languages l' for the FSM			
	Frequency	Transmission	Reflection
flux1:	0.1	-4.23E-08	4.05E-07
flux1:	0.10101	-6.33E-08	7.63E-07
flux1:	0.10202	-9.20E-08	1.40E-06
flux1:	0.10303	-1.33E-07	2.48E-06
flux1:	0.10404	-1.94E-07	4.18E-06
flux1:	0.105051	-2.88E-07	6.76E-06
flux1:	0.106061	-4.36E-07	1.05E-05
flux1:	0.107071	-6.66E-07	1.59E-05
flux1:	0.108081	-1.01E-06	2.34E-05
flux1:	0.109091	-1.53E-06	3.38E-05
flux1:	0.110101	-2.26E-06	4.81E-05
flux1:	0.111111	-3.30E-06	6.76E-05
flux1:	0.112121	-4.76E-06	9.38E-05
flux1:	0.113131	-6.79E-06	1.28E-04
flux1:	0.114141	-9.62E-06	1.72E-04
flux1:	0.115152	-1.36E-05	2.27E-04
flux1:	0.116162	-1.92E-05	2.95E-04
flux1:	0.117172	-2.71E-05	3.74E-04
flux1:	0.118182	-3.81E-05	4.67E-04
flux1:	0.119192	-5.32E-05	5.70E-04
flux1:	0.120202	-7.40E-05	6.83E-04
flux1:	0.121212	-1.02E-04	8.01E-04
flux1:	0.122222	-1.40E-04	9.19E-04
flux1:	0.123232	-1.90E-04	0.001029
flux1:	0.124242	-2.56E-04	0.001119
flux1:	0.125253	-3.42E-04	0.00118
flux1:	0.126263	-4.55E-04	0.001205
flux1:	0.127273	-6.01E-04	0.001193
flux1:	0.128283	-7.87E-04	0.001164
flux1:	0.129293	-0.0010206	0.001157
flux1:	0.130303	-0.0013108	0.001247
flux1:	0.131313	-0.0016636	0.001546
flux1:	0.132323	-0.0020838	0.002201
flux1:	0.133333	-0.002573	0.003385
flux1:	0.134343	-0.0031292	0.005286
flux1:	0.135354	-0.0037466	0.008072
flux1:	0.136364	-0.0044158	0.011872
flux1:	0.137374	-0.005124	0.016739
flux1:	0.138384	-0.0058567	0.022632
flux1:	0.139394	-0.0065986	0.029403
flux1:	0.140404	-0.0073349	0.036801
flux1:	0.141414	-0.0080526	0.044489
flux1:	0.142424	-0.0087411	0.05208
flux1:	0.143434	-0.0093923	0.059173
flux1:	0.144444	-0.0100013	0.065388
flux1:	0.145455	-0.0105651	0.070407
flux1:	0.146465	-0.0110827	0.073984
flux1:	0.147475	-0.011554	0.075962
flux1:	0.148485	-0.0119795	0.076264
flux1:	0.149495	-0.012359	0.07489
flux1:	0.150505	-0.0126916	0.071906
flux1:	0.151515	-0.0129748	0.06744
flux1:	0.152525	-0.0132038	0.061676
flux1:	0.153535	-0.013372	0.054855
flux1:	0.154545	-0.0134707	0.047272
flux1:	0.155556	-0.0134901	0.039264
flux1:	0.156566	-0.0134201	0.031194
flux1:	0.157576	-0.0132524	0.023421
flux1:	0.158586	-0.0129819	0.016269
flux1:	0.159596	-0.012608	0.010004
flux1:	0.160606	-0.0121359	0.004803
flux1:	0.161616	-0.0115763	7.53E-04
flux1:	0.162626	-0.0109448	-0.00215
flux1:	0.163636	-0.0102603	-0.00399
flux1:	0.164646	-0.0095427	-0.0049
flux1:	0.165657	-0.0088109	-0.00505
flux1:	0.166667	-0.0080811	-0.00459
flux1:	0.167677	-0.0073652	-0.00372
flux1:	0.168687	-0.0066713	-0.00258
flux1:	0.169697	-0.0060035	-0.00131

flux1:	0.170707	-0.0053635	-4.50E-05
flux1:	0.171717	-0.004752	0.001117
flux1:	0.172727	-0.0041699	0.002092

APPENDIX -II			
MEEP simulation: circular waveguide with central groove or cylinder flux as languages l'' for the FSM			
	Frequency	Transmission	Reflection
flux1:	0.1	-4.11E-08	4.22E-07
flux1:	0.1010101	-6.26E-08	8.02E-07
flux1:	0.1020202	-9.19E-08	1.45E-06
flux1:	0.1030303	-1.33E-07	2.51E-06
flux1:	0.1040404	-1.92E-07	4.18E-06
flux1:	0.10505051	-2.82E-07	6.71E-06
flux1:	0.10606061	-4.23E-07	1.05E-05
flux1:	0.10707071	-6.40E-07	1.59E-05
flux1:	0.10808081	-9.71E-07	2.35E-05
flux1:	0.10909091	-1.46E-06	3.43E-05
flux1:	0.11010101	-2.17E-06	4.91E-05
flux1:	0.11111111	-3.18E-06	6.92E-05
flux1:	0.11212121	-4.58E-06	9.61E-05
flux1:	0.11313131	-6.54E-06	1.31E-04
flux1:	0.11414141	-9.26E-06	1.77E-04
flux1:	0.11515152	-1.31E-05	2.34E-04
flux1:	0.11616162	-1.84E-05	3.05E-04
flux1:	0.11717172	-2.58E-05	3.91E-04
flux1:	0.11818182	-3.62E-05	4.91E-04
flux1:	0.11919192	-5.05E-05	6.06E-04
flux1:	0.12020202	-7.01E-05	7.34E-04
flux1:	0.12121212	-9.67E-05	8.72E-04
flux1:	0.12222222	-1.32E-04	0.001013
flux1:	0.12323232	-1.79E-04	0.001151
flux1:	0.12424242	-2.42E-04	0.001276
flux1:	0.12525253	-3.23E-04	0.001377
flux1:	0.12626263	-4.29E-04	0.001444
flux1:	0.12727273	-5.66E-04	0.001472
flux1:	0.12828283	-7.42E-04	0.001471
flux1:	0.12929293	-9.64E-04	0.001465
flux1:	0.13030303	-0.0012412	0.00151
flux1:	0.13131313	-0.0015811	0.001696
flux1:	0.13232323	-0.0019901	0.00215
flux1:	0.13333333	-0.002472	0.003034
flux1:	0.13434343	-0.003027	0.004532
flux1:	0.13535354	-0.0036515	0.006828

flux1:	0.13636364	-0.004338	0.010081
flux1:	0.13737374	-0.0050748	0.014388
flux1:	0.13838384	-0.0058475	0.019763
flux1:	0.13939394	-0.0066396	0.026111
flux1:	0.14040404	-0.0074343	0.033225
flux1:	0.14141414	-0.0082153	0.040798
flux1:	0.14242424	-0.0089686	0.048451
flux1:	0.14343434	-0.0096827	0.055772
flux1:	0.14444444	-0.0103492	0.062354
flux1:	0.14545455	-0.010963	0.067837
flux1:	0.14646465	-0.0115216	0.071936
flux1:	0.14747475	-0.0120245	0.074453
flux1:	0.14848485	-0.0124723	0.075282
flux1:	0.14949495	-0.012866	0.0744
flux1:	0.15050505	-0.0132053	0.071859
flux1:	0.15151515	-0.0134887	0.067779
flux1:	0.15252525	-0.013712	0.062342
flux1:	0.15353535	-0.0138691	0.055786
flux1:	0.15454545	-0.0139513	0.048407
flux1:	0.15555556	-0.013949	0.040542
flux1:	0.15656566	-0.0138527	0.032556
flux1:	0.15757576	-0.0136547	0.024815
flux1:	0.15858586	-0.0133507	0.017651
flux1:	0.15959596	-0.0129414	0.011336
flux1:	0.16060606	-0.012433	0.006061
flux1:	0.16161616	-0.0118376	0.001918
flux1:	0.16262626	-0.0111716	-0.00109
flux1:	0.16363636	-0.0104544	-0.00304
flux1:	0.16464646	-0.0097065	-0.00406
flux1:	0.16565657	-0.0089468	-0.00431
flux1:	0.16666667	-0.0081916	-0.00396

Modeling the Design of Plasmonic Biosensor Device by using Abstract Finite State Machine Model and FDTD Based MEEP Tool

flux1:	0.16767677	-0.0074528	-0.00319
flux1:	0.16868687	-0.0067383	-0.00214
flux1:	0.16969697	-0.0060524	-9.57E-04
flux1:	0.17070707	-0.0053968	2.38E-04
flux1:	0.17171717	-0.0047722	0.001341
flux1:	0.17272727	-0.0041794	0.002269
flux1:	0.17373737	-0.0036201	0.002964
flux1:	0.17474747	-0.0030972	0.003397
flux1:	0.17575758	-0.0026144	0.003568
flux1:	0.17676768	-0.0021759	0.003502
flux1:	0.17777778	-0.001785	0.003246
flux1:	0.17878788	-0.0014438	0.002859
flux1:	0.17979798	-0.0011526	0.0024
flux1:	0.18080808	-9.10E-04	0.001925
flux1:	0.18181818	-7.11E-04	0.001475
flux1:	0.18282828	-5.52E-04	0.001081
flux1:	0.18383838	-4.26E-04	7.55E-04
flux1:	0.18484848	-3.28E-04	5.00E-04
flux1:	0.18585859	-2.52E-04	3.10E-04
flux1:	0.18686869	-1.93E-04	1.77E-04
flux1:	0.18787879	-1.47E-04	8.77E-05
flux1:	0.18888889	-1.12E-04	3.19E-05
flux1:	0.18989899	-8.37E-05	-8.93E-08
flux1:	0.19090909	-6.21E-05	-1.58E-05
flux1:	0.19191919	-4.53E-05	-2.11E-05
flux1:	0.19292929	-3.25E-05	-2.04E-05
flux1:	0.19393939	-2.29E-05	-1.67E-05
flux1:	0.19494949	-1.59E-05	-1.20E-05
flux1:	0.1959596	-1.08E-05	-7.78E-06
flux1:	0.1969697	-7.28E-06	-4.46E-06
flux1:	0.1979798	-4.85E-06	-2.21E-06
flux1:	0.1989899	-3.21E-06	-9.08E-07
flux1:	0.2	-2.11E-06	-2.72E-07

REFERENCES

1. S. Vashist, "Point-of-Care Diagnostics: Recent Advances and Trends," *Biosensors*, 7, (2017) [doi: 10.3390/bios7040062].
2. Yao, B. Yi, J. Xiao and Z. Li, "Surface Plasmon Resonance Biosensors and its Application," *1st International Conference on Bioinformatics and Biomedical Engineering*, (2007) [doi: 10.1109/icbbe.2007.270].
3. W. Gu, L. Peng, S. Lai, and Y. Wu, "The application of surface plasmon polariton effect in photonic integration," *14th International Conference on Optical Communications and Networks (ICOCN),* (2015) [doi: 10.1109/icocn.2015.7203753].
4. K. Le, Q. Ngo and T. Nguyen, "Nanostructured Metal–Insulator–Metal Metamaterials for Refractive Index Biosensing Applications: Design, Fabrication, and Characterization," *IEEE Journal of Selected Topics in Quantum Electronics, 23(2),* 388-393 (2017) [doi:10.1109/jstqe.2016.2615944].
5. J. Fiala, P. Kwiecien and I. Richter, "Physics and design possibilities of plasmonic-based fishnet metamaterial structures," *18th Czech-Polish-Slovak Optical Conference on Wave and Quantum Aspects of Contemporary Optics*, (2012) [doi:10.1117/12.2006862].
6. R. Yahiaoui, A. C. Strikwerda, and P. U. Jepsen, "Terahertz Plasmonic structure with enhanced sensing capabilities," *IEEE Sensors Journal*, 16(8), 2484–2488 [doi:10.1109/jsen.2016.2521708].
7. M. Nagel, P. Bolivar, and H. Kurz, "Modular parallel-plate THz components for cost-efficient biosensing systems," *Semicon. Sci. Technol.,* 20, S281-S285 (2005).
8. X. Liang, A. Q. Liu, X. M. Zhang, P. Yap, T. C. Ayi, and H. S. Yoon, "Determination of refractive index for single living cell using integrated biochip," *Solid-State Sensors, Actuators and Microsystems*, 2, 1712-1715 (2005) [doi:10.1109/SENSOR.2005.1497421].
9. X. Jin, X. Huang, J. Tao, X. Lin and Q. Zhang, "A Novel Nanometeric Plasmonic Refractive Index Sensor," *IEEE Transactions on Nanotechnology*, 9(2), 134-137 (2010) [doi:10.1109/tnano.2009.2038909].
10. Y. Liu et al., "Theoretical Design of Plasmonic Refractive Index Sensor Based on the Fixed Band Detection," *IEEE Journal of Selected Topics in Quantum Electronics*, 25(2), 1-6 (2019) [doi:10.1109/jstqe.2018.2827661].
11. S. Chan, Y. Li, L. Rothberg, B. Miller and P. Fauchet, "Nanoscale silicon microcavities for biosensing," *Materials Science and Engineering: C*, 15(1-2), 277-282 (2001) [doi: 10.1016/s0928-4931(01)00219-3].
12. A. Syahir, K. Usui, K. Tomizaki, K. Kajikawa and H. Mihara," Label and Label-Free Detection Techniques for Protein Microarrays," *Microarrays*, 4(2), 228-244 (2015) [doi:10.3390/microarrays4020228].
13. A. F. Oskooi, D. Roundy, M. Ibanescu, P. Bermel, J. D. Joannoopoulos, and S. G. Johnson, "MEEP: A flexible freesoftware package for electromagnetic simulations by the FDTD method," *Computer Physics Communications*, 181, 87-702 (2010) [doi: 10.1016/j.cpc.2009.11.008].
14. H. Pereira, J. Rocha, L. Caballero and O. Neto, "Photonic crystal design tool," *32nd Symposium on Microelectronics Technology and Devices (SBMicro)*, (2017) [doi: 10.1109/sbmicro.2017.8113020].
15. N. Chiu, T. Wey, C. Yu, T. Hsiao and C. Lin, "Advanced Plasmonic Biosensing Devices and Automation Systems for Disease Diagnostic and Drug Screening Applications", *Eighth International Conference on Intelligent Systems Design and Applications*, (2008) [doi:10.1109/isda.2008.39].
16. Miró, Jesús M., and Alfonso Rodríguez-Patón. "Biomolecular computing devices in synthetic biology," *International Journal of Nanotechnology and Molecular Computation (IJNMC)*, 2(2), 47-64 (2010).
17. Wang, Zhen-Gang, et al. "All-DNA finite-state automata with finite memory," *Proceedings of the National Academy of Sciences*, (2010).
18. Ramachandran, P., & Varoquaux, G., "Mayavi: 3D visualization of scientific data," Computing in Science & Engineering, 13(2), 40–51(2011) [doi:10.1109/mcse.2011.35].
19. Folk, M., McGrath, R. E., & Yeager, N. (n.d.). "HDF: An update and future directions," *IEEE 1999 International Geoscience and Remote Sensing Symposium. IGARSS'99* (Cat. No.99CH36293), (1999) [doi:10.1109/igarss.1999.773469].